Available online at www.sciencedirect.com
SCIENCE DIRECT®
Journal of Chromatography A, 1065 (2005) 231–237
JOURNAL OF CHROMATOGRAPHY A
www.elsevier.com/locate/chroma

Effect of injected sample amount on the shape of chromatographic peaks under condition of linear partition isotherm

S. Vezzani, P. Moretti, R. Peri, G. Castello*

Università di Genova, Dipartimento di Chimica e Chimica Industriale, Via Dodecaneso 31, Genova I-16146, Italy

Received 21 October 2004; received in revised form 9 December 2004; accepted 16 December 2004

Abstract

In a previous paper a model function was tested in order to approximate the peak shape obtained on non-polar column by injecting different compounds. The simulation of the symmetrical or non-symmetrical shape of gas chromatographic peaks was satisfactory. In this paper, the influence of the amount of injected substance was investigated at different values of inlet pressure and carrier gas velocity, in order to evaluate the relative contribution to the total peak area and shape of the symmetrical distribution due to partition phenomena and of the non-symmetrical and tailing distribution due to adsorption–desorption kinetics. The effect of the molecular mass and of the chain length of compounds belonging to the homologous series of 1-alcohols and *n*-alkanes on the adsorption phenomena was evaluated.

Keywords: Capillary columns; Inlet pressure; Sample concentration; Peak shape; Peak symmetry; Partition isotherm; Adsorption; Mathematical models

1. Introduction

The model proposed previously [1] for the evaluation of the shape of chromatographic peaks and the prediction of the retention time and width at different pressure values was found to yield accurate results when the parameters of the function describing the behaviour of the gas chromatographic signal are known. Several mathematical models describing peak shape are found in the literature [2–4], but no one of them takes into account the effect of the amount of analyte on the accuracy of the prediction. For sake of simplicity, the proposed model separates the contribution of the two main phenomena simultaneously influencing the peak shape: the partition between the carrier gas and the liquid or polymeric stationary phase and the adsorption–desorption on the inert support or on the inner walls of the capillary column. The first contribution leads to a symmetrical distribution of the analyte due to axial diffusion, resistance to mass transfer in the mobile phase and in the stationary phase and unevenness of flow pattern. The adsorption–desorption kinetics [5–9] and the non-linearity of the partition isotherm [10] both lead to non-symmetrical distribution of the analyte and to peaks showing more or less tailing. The adsorption leads to peaks with sharp front and very slow and near exponential decrease of the signal, whereas the non-linear partition isotherm causes asymmetry starting from the top of the peak, with different slope of the front and rear trace. When the amount of injected substance is very small and near to the infinite dilution condition, one can suppose that the partition isotherm is linear also when the polarities of the analyte and of the stationary phase are different, and therefore the adsorption remains the unique source of tailing. The model does not take into account separately other phenomena, which contribute to the peak shape: the diffusion kinetics into the liquid phase, being a reversible mechanism, contributes to the symmetrical part of the peak, whereas phenomena occurring at the gas–liquid and liquid–solid interface, the temporal distortion effects [11,12] the extra-column effects [13] and other non reversible interactions generate an exponential decay of the peak broadening, which is added to the gas–solid adsorption phenomenon. However, the fitting of the experimental shape of the peaks obtained by the sum of the partition and adsorption contributes is very good showing that the con-

* Corresponding author. Tel.: +39 010 353 6176; fax: +39 010 353 6190.
E-mail address: castello@chimica.unige.it (G. Castello).

0021-9673/$ – see front matter © 2004 Elsevier B.V. All rights reserved.
doi:10.1016/j.chroma.2004.12.048

tribution of other phenomena is small and can be neglected or is included into the two main mechanisms, and that the simplified model well reconstructs the shape of tailing peaks without requiring complicated convolution integrals.

In the present work the mathematical model described previously was applied in order to simulate the peak shape obtained by injecting different amounts of sample in isothermal conditions but with different inlet pressure and carrier gas velocity. The simulated peak shape was compared with the experimental results. Compounds of different polarity, belonging to the homologous series of *n*-alkanes and 1-alcohols, were used as probes and the different contribution of the partition and adsorption phenomena was evaluated with respect to the different amounts of injected sample.

2. Theory

In a previously published paper [1] a mathematical model was described which permits to predict the shape of a chromatographic peak, taking into account the phenomena occurring during the elution of a given compound along the gas chromatographic column. When solute–solvent partition only is present in a capillary column and the analyte and the stationary phase are mutually soluble, the phenomena are: longitudinal diffusion, resistance to mass transfer between gas and liquid phase, convective mixing due to radial diffusion from the centre to the walls of the column. These effects are stocastic or reversible, and their sum yields a symmetrical distribution of the signal intensity. When the analyte and the liquid phase are not completely miscible, a non-linear partition isotherm is observed and the concentration of the analyte in the liquid phase does not increase proportionally to its concentration in the mobile gas phase; in this instance, the peak shows a steep front and a flat back and this kind of asymmetry starts from the peak top. Another effect of the non-linear partition isotherm is that the retention time measured at the peak apex decreases when the injected sample amount is great. When the injected amount is small, the first tract of the partition isotherm is linear also when the analyte and the liquid phase are not completely miscible and this is shown by the symmetrical shape of the peak and by the reproducibility of the retention time.

Often, when polar compounds are analysed, another phenomenon influences the peak shape causing a delay in the elution of a small amount of the analyte with respect of the retention time of the bulk, leading to a peak symmetrical in the upper part of the plot but showing a tail in the lower part of its back. This may be due to adsorption which takes place at the gas/solid interface when the liquid phase does not cover completely the capillary column wall (or the inert support in packed columns) or at the liquid/solid interface because a fraction of the analyte permeates through the liquid film and reacts with the active centres of the support or of the capillary wall. The interaction is mainly due to the formation of hydrogen bonds or other polar chemical bonding between the analyte (adsorbate) and the solid surface (adsorbent). The overall effect of the adsorption is to subtract an amount of the analyte (solute) to the partition interactions with the liquid stationary phase (solvent). When adsorption is present, the peak shape can be reconstructed as the sum of two contributes: a symmetrical or asymmetrical "from the top" behaviour, depending on the linear or non-linear solute–solvent partition isotherm, and a near vertical front, followed by a slow exponential decrease, due to adsoption–desorption kinetics. This simplified model fits very well the experimental peak shape and does not require separate calculation of the effects of other phenomena, as pointed out in Section 1, thus reducing the length of the procedure.

As shown previously [1] the final equation of the model which takes into account the sum of the partition and adsorption–desorption contribution is:

$$y(t) = y_0 \exp\left\{-\frac{1}{2(1-r^2)}\left[\frac{(t-t_R)^2}{\sigma_1^2} - 2r\frac{(t-t_R)\ln(1+\gamma(t-t_R))}{\sigma_1\sigma_2} + \frac{[\ln(1+\gamma(t-t_R))]^2}{\sigma_2^2}\right]\right\} + y_G \exp\left[-\frac{(t-t_R)^2}{2\sigma_G^2}\right] \quad (1)$$

where $y(t)$ is the signal intensity at the column outlet at the time t, y_0 is the peak height due to the fraction of sample involved in the adsorption phenomenon, r the correlation coefficient between symmetrical partition distribution and asymmetrical adsorption distribution, t_R is the time corresponding to the maximum intensity of the detector signal, σ_1 the dispersion of the symmetrical partition distribution, σ_2 the dispersion of the asymmetric adsorption distribution, γ is a parameter connected to the asymmetry value, y_G, σ_G are the peak height and the dispersion, respectively, of the symmetrical partition due to the fraction of the injected amount of sample not involved in the adsorption phenomenon, Eq. (1) can be summarised as:

$$y(t) = y_{ads}(t) + y_{part}(t) \quad (2)$$

where $y_{ads}(t)$ is the contribution of the adsorption–desorption distribution between the carrier gas and the active sites of the column wall and $y_{part}(t)$ is the contribution of the gas–liquid partition between the carrier gas and the layer of liquid or polymeric stationary phase not involved in the adsorption phenomenon.

The relative contribution of the two phenomena, in terms of area, can be written as:

$$R_{ads} = \frac{A_{ads}}{A_{cal}} \quad (3)$$

and

$$R_{\text{part}} = \frac{A_{\text{part}}}{A_{\text{cal}}} \quad (4)$$

where A_{cal} is the total peak area calculated with the mathematical model of Eq. (1), A_{ads} is the peak area due to the adsorption–desorption phenomenon, A_{part} is the peak area due to the partition phenomenon only. The aim of this work was to evaluate how the importance of the two phenomena depends on the different amount of injected substance and of the column inlet pressure.

3. Experimental

The determination of the retention times and peak shape of reference mixtures containing non-polar and polar compounds was made by using a non-polar poly(dimethylsiloxane) DB-1 capillary column (J&W Scientific, Folsom, CA, USA) with a length of 30 m × 0.32 mm I.D., phase thickness 0.25 μm, which was installed in a Varian model 3800 gas chromatograph (Varian, Palo Alto, CA, USA) equipped with a split–splitless injector and a flame ionisation detector. Helium was used as the carrier gas. The split ratio was 1/20. The inlet pressure of the column was controlled and measured by the electronic hardware of the gas chromatograph with an accuracy of ±0.1 psi, unit used by the pressure programmer of the instrument. Being 1 psi equivalent to 6894.76 Pa, all the psi values were converted to kPa, and rounded up to the first decimal figure. The accuracy of the pressure automatic measurement is therefore ±0.7 kPa. Samples containing several terms of the homologous series of *n*-alkanes and of straight chain 1-alcohols were injected (1 μl) as solution raging from about 35 to about 1000 mg/1 concentration of every compound in *n*-hexane. The absolute amount of each compound injected ranged between about 1.75 to about 50 ng, depending on the density of the compound. The analyses were carried out at 130 °C in the inlet pressure range 51.7–172.4 kPa at 17.2 kPa interval (7.5–25 psig at 2.5 psi interval). The signal value was sampled by the data system (Varian Star) at an interval of 0.1 s for all the analyses, independent on the retention time and peak width.

4. Result and discussion

Table 1 shows the retention times, t_R, the experimental peak areas, A_{exp}, the total peak area calculated with Eq. (1), A_{cal}, and the relative percent error between experimental and calculated area, $E\%_{\text{rel}} = 100(A_{\text{exp}} - A_{\text{cal}})/A_{\text{exp}}$, of 1-alcohols with 9–12 carbon atoms and *n*-alkanes with 12–15 carbon atoms at 130 °C and at the inlet pressure of 51.7, 120.7, 172.4 kPa. Compounds with a smaller and a greater number of carbon atoms were tested for both homologous series, but at the selected temperature and pressure values the lightest compounds were eluted on the tail of the solvent peak, and the peaks of the heaviest ones were too large and flat and affected by the baseline noise; the accurate measurement of the area and of the peak shape was therefore subjected to large errors. However, the considered range of carbon atoms number and of the retention time was great enough to investigate the behaviour of compounds with different molecular mass and boiling points.

Table 1
Retention times, t_R, experimental peak areas, A_{exp}, peak areas calculated with the mathematical model, A_{cal}, relative percent error between experimental and calculated area, $E\%_{\text{rel}} = 100(A_{\text{exp}} - A_{\text{cal}})/A_{\text{exp}}$, of 1-alcohols with 9–12 carbon atoms and *n*-alkanes with 12–15 carbon atoms at 130 °C and at the inlet pressure of 51.7, 120.7, 172.4 kPa

P (kPa)	Compound	t_R	A_{exp}	A_{cal}	$E\%_{\text{rel}}$
51.7	1-C9OH	4.232	9682	9698	−0.17
120.7		1.890	8020	7942	0.97
172.4		1.355	9292	9257	0.38
51.7	1-C10OH	5.697	8615	8735	−1.39
120.7		2.542	7080	7102	−0.32
172.4		1.823	8305	8248	0.70
51.7	1-C11OH	8.198	8535	8634	−1.16
120.7		3.655	7644	7586	0.76
172.4		2.623	8343	8252	1.09
51.7	1-C12OH	12.466	12249	12259	−0.08
120.7		6.582	10875	10867	0.07
172.4		3.985	11940	11931	0.07
51.7	*n*-C12	4.743	11399	11461	−0.54
120.7		2.118	9263	9268	−0.06
172.4		1.518	11940	11931	0.07
51.7	*n*-C13	6.547	11080	11106	−0.24
120.7		2.918	9353	9426	−0.78
172.4		2.093	10402	10392	0.09
51.7	*n*-C14	9.609	11346	11466	−1.05
120.7		4.278	9826	9826	0.00
172.4		3.070	10497	10500	−0.02
51.7	*n*-C15	14.798	10602	10576	0.24
120.7		6.582	10431	10392	0.37
172.4		4.723	11748	11734	0.12

The mathematical model described was used in order to obtain the best fit of the peak shape of the compounds belonging to the homologous series of *n*-alkanes and 1-alcohols and to calculate the total area, the symmetrical peak area due to the partition and the tailing portion due to the adsorption–desorption mechanism, in isothermal conditions and at various inlet pressure values and amount of injected sample. Fig. 1 shows the experimental data, the simulated peak shape of *n*-tetradecane analysed at 130 °C and the contribution of the two phenomena at the inlet pressure of 86.2 kPa and at the concentration of 191 mg/l. Fig. 2 shows the experimental data, the simulated peak shape of the 1-undecanol analysed at 130 °C and the contribution of the two phenomena at the inlet pressure of 155.1 kPa and at the concentration of 207 mg/l. No measurable adsorption or other minor effects causing peak asymmetry were observed for hydrocarbons whereas the influence of the gas–solid interaction due

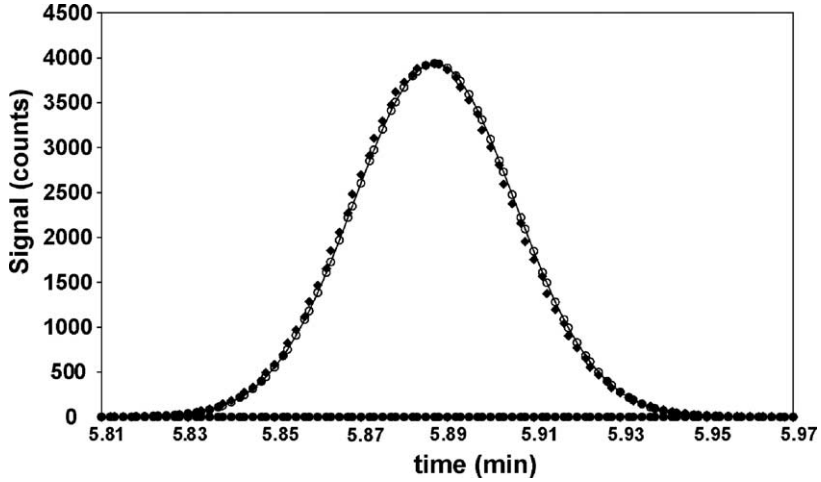

Fig. 1. Peak of *n*-tetradecane (concentration 191 mg/l) at 130 °C and 86.2 kPa. Black rhombs: experimental data; line: simulated peak shape; white circles: Gaussian distribution curve; black circles: contribution of the adsorption.

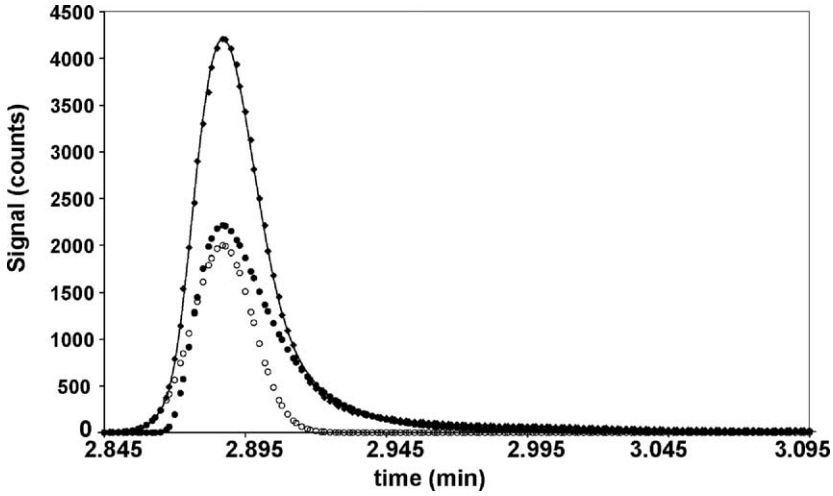

Fig. 2. Peak of 1-undecanol (concentration 207 mg/l) at 130 °C and 155.1 kPa. Black rhombs: experimental data; line: simulated peak shape; white circles: Gaussian distribution curve; black circles: contribution of the adsorption.

to the hydrogen bonding of the alcohols with the silanol and siloxane groups of the column wall greatly contributes to the total peak area. In the investigated ranges of carbon atoms number the behaviour of all the tested compounds of each homologous series was very similar. Therefore, the evaluations reported below are referred to two compounds with similar retention times lying near to the centre of the investigated range: *n*-tetradecane and 1-undecanol. The behaviour of all the other compounds listed in Table 1 is very similar to that of the two selected probes.

Tables 2–5 show the values of A_{cal}, $E\%_{rel}$, A_{part} and R_{part} for 1-undecanol and *n*-tetradecane measured at eight inlet pressure values and with four concentrations of the analytes. The amount of sample, calculated by taking into account the injected volume and the splitting ratio, is also shown. The definitions of $E\%_{rel}$ and A_{cal} were given above, R_{part} is the ratio between the area due to the partition, A_{part}, calculated with the second term of Eq. (1) and the calculated total area A_{cal} (the corresponding term R_{ads} can be calculated as $1 - R_{part}$). The approximation of the calculated peak area to the experimental one is fair, as shown by the small values of the relative percent error. It was found, however, that the matching of calculated to experimental peak area and shape decreases with increasing

Table 2
A_{cal}, $E\%_{rel}$, A_{part} and R_{part} values at different inlet pressure for 1-undecanol and *n*-tetradecane (concentration 41 and 38 mg/l, averaged injected amount 2.05 and 1.9 ng, respectively)

P (kPa)	1-C11OH, C_1 = 41 mg/l				*n*-C14, C_1 = 38 mg/l			
	A_{cal}	$E\%_{rel}$	A_{part}	R_{part}	A_{cal}	$E\%_{rel}$	A_{part}	R_{part}
172.4	1956	0.01	783	0.40	2362	−0.12	2351	1.00
155.1	1969	−0.02	928	0.47	2357	−0.02	2357	1.00
137.9	2105	0.38	940	0.45	2120	−1.19	2102	0.99
120.7	1710	−0.49	701	0.41	2483	0.05	2483	1.00
103.4	1658	−0.32	630	0.38	2266	1.19	2239	0.99
86.2	1576	−0.19	519	0.33	2162	0.09	2162	1.00
68.9	1755	−0.24	491	0.28	2384	−0.18	2384	1.00
51.7	1299	−0.58	304	0.23	2103	−0.13	2061	0.98

Column temperature 130 °C.

Table 3
A_{cal}, $E\%_{rel}$, A_{part} and R_{part} values at different inlet pressure for 1-undecanol and *n*-tetradecane (concentration 83 and 76 mg/l, average injected amount 4.15 and 3.8 ng, respectively)

P (kPa)	1-C11OH, C_1 = 83 mg/1				*n*-C14, C_1 = 76 mg/l			
	A_{cal}	$E\%_{rel}$	A_{part}	R_{part}	A_{cal}	$E\%_{rel}$	A_{part}	R_{part}
172.4	3416	1.17	1318	0.39	4196	−0.08	4191	1.00
155.1	2976	1.30	1182	0.40	4044	−0.55	4011	0.99
137.9	3281	−0.17	1445	0.44	4237	0.62	4237	1.00
120.7	3613	−0.12	1517	0.42	4467	−0.20	4464	1.00
103.4	3010	−0.44	1128	0.37	3793	0.52	3777	1.00
86.2	3810	−0.30	1261	0.33	4386	−0.95	4377	1.00
68.9	3323	−0.49	928	0.28	3872	0.33	3831	0.99
51.7	2783	0.73	638	0.23	3673	0.00	3670	1.00

Column temperature 130 °C.

Table 4
A_{cal}, $E\%_{rel}$, A_{part} and R_{part} values at different inlet pressure for 1-undecanol and *n*-tetradecane (concentration 207 and 191 mg/l, averaged injected amount 10.35 and 9.55 ng, respectively)

P (kPa)	1-C11OH, C_1 = 207 mg/l				*n*-C14, C_1 = 191 mg/l			
	A_{cal}	$E\%_{rel}$	A_{part}	R_{part}	A_{cal}	$E\%_{rel}$	A_{part}	R_{part}
172.4	8252	1.09	2917	0.35	10500	−0.02	10497	1.00
155.1	8077	1.50	3211	0.40	9751	−0.18	9751	1.00
137.9	6907	1.09	2856	0.41	9763	−0.19	9754	1.00
120.7	7586	0.76	3319	0.44	9826	0.00	9825	1.00
103.4	7592	0.11	2969	0.39	9760	−0.07	9760	1.00
86.2	8301	−0.07	2941	0.35	11062	0.25	11050	1.00
68.9	6528	−0.45	2098	0.32	9347	0.11	9347	1.00
51.7	8634	−1.16	2418	0.28	11466	−1.05	11458	1.00

Column temperature 130 °C.

baseline drift and noise. Clean and well conditioned columns, stable temperature control; carrier gas purity and low detector noise enhance therefore the results of the procedure. The R_{part} ratio is much greater for *n*-alkanes than for 1-alcohols, as the shape of the peaks of the non-polar compounds is very symmetrical and can be considered as a near-Gaussian distribution (Fig. 1), whereas the alcohols show non-symmetrical peaks (Fig. 2) mainly at low sample concentration. The contribution of adsorption is therefore negligible for non-polar compounds as hydrocarbons, and the amount of total area due to this phenomenon, A_{ads}, is very small as can be seen by the

Table 5
A_{cal}, $E\%_{rel}$, A_{part} and R_{part} values at different inlet pressure for 1-undecanol and *n*-tetradecane (concentration 1037 and 954 mg/l, averaged injected amount 51.85 and 47.7 ng, respectively)

P (kPa)	1-C11OH, C_1 = 1037 mg/l				*n*-C14, C_1 = 954 mg/l			
	A_{cal}	$E\%_{rel}$	A_{part}	R_{part}	A_{cal}	$E\%_{rel}$	A_{part}	R_{part}
172.4	44753	−0.14	32222	0.72	51547	−0.50	51497	1.00
155.1	48392	0.06	34648	0.72	54746	0.17	54626	1.00
137.9	42863	0.71	29575	0.69	50154	0.32	50119	1.00
120.7	48631	0.89	33268	0.68	55835	0.42	55835	1.00
103.4	41291	0.10	27730	0.67	49518	0.04	49166	0.99
86.2	46591	−0.33	31682	0.68	53769	0.31	53759	1.00
68.9	41901	−0.48	29172	0.70	49183	0.22	49183	1.00
51.7	37802	0.89	26237	0.69	45389	0.18	45227	1.00

Column temperature 130 °C.

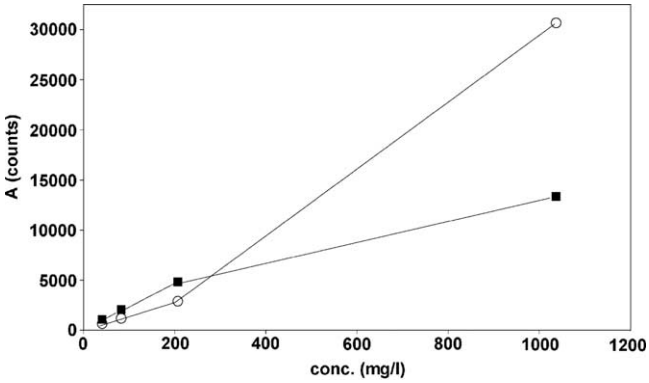

Fig. 3. Average of the values of the contribution to the total peak area of 1-undecanol of the adsorption, A_{ads} (black squares) and of the partition, A_{part} (white circles), as a function of the injected sample amount.

difference between the A_{cal} and A_{part} values in Tables 2–5. As a consequence, the values of R_{part} at different concentrations of *n*-tetradecane as a function of the inlet pressure are very close to unit for all the tested conditions of pressure and injected amount, according to the symmetrical shape of the alkane peak (Fig. 1).

As shown in Fig. 2, the total area of 1-undecanol peak is formed by the sum of the adsorption, A_{ads}, and of the partition, A_{part}, contributions. Up to the concentration of the injected sample of about 200 mg/l (amount about 10 ng) the A_{ads} is greater than the A_{part}, and both contributes increase linearly with the sample concentration, as shown by the trend of the average values of the peak areas A_{ads} and A_{part}, reported in Fig. 3. Up to the sample concentration of about 200 mg/l (injected amount about 10 ng) the behaviour is linear (correlation coefficient R^2 close to 1). When the injected amount increases, the partition contribution increases with respect of the adsorption, as shown by the inversion of the lines in Fig. 3. At the highest sample concentration, also the R_{ads} and R_{part} values show an inversion because, when a large amount of analyte is available, all the active sites are saturated, further adsorption is inhibited, the asymmetric peak area correlated with it cannot increase and the partition mechanism prevails. However, the greatest amounts of analyte injected in our experiments were small enough to avoid the saturation of the liquid phase, as shown by the constant values of the retention times when the sample concentration increases (see Fig. 4, where the experimental peak shape of 1-undecanol for sample concentrations of 41, 83, 207 and 1037 mg/l is shown). Linear partition isotherms are therefore present at every flow rate, and the peak contribution of the partition does not show "from the top" asymmetry.

Fig. 5 shows the behaviour of the ratios R_{part} for 1-undecanol at various concentrations as a function of inlet pressure. The adsorption–desorption is predominant at low sample concentrations, as shown in Fig. 3. At low pressure values, i.e. small carrier flow velocity, the analyte molecules have a long time to reach the equilibrium between the carrier gas and the liquid phase and to permeate and be adsorbed

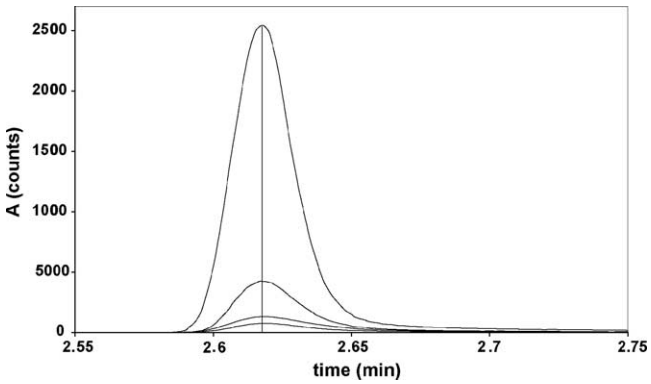

Fig. 4. Peak shape (experimental values) of the 1-undecanol peak at various concentrations of the injected sample. The retention time and the peak symmetry do not change with increasing sample amount, showing linear partition isotherm and no saturation of the liquid phase.

on the active sites of the column wall; as a consequence the contribution of adsorption to the total peak area is great. With increasing carrier gas velocity, the effect of partition increases with respect of the adsorption and a maximum value is reached at an inlet pressure greater for increasing sample amount. When inlet pressure and carrier gas velocity increase further, the contribution of the adsorption mechanism increases again. This may be due to the fact that the motion of the gas phase is so fast that the molecules adsorbed on the wall active surface are released with increasing delay with respect of the bulk of the peak subjected to partition only and therefore the peak tailing increases. This effect may be compared with the increasing influence of the resistance to the mass transfer between stationary and mobile phase with increasing flow velocity, responsible of the right climbing portion of the classical Van Deemter–Jones plot. The behaviour of the plot representing the highest sample concentration (1037 mg/l) is quite different from that observed at lower sample concentration, because the great amount of analyte saturates the adsorbing sites, the partition mechanism increases faster than adsorption, and the values of R_{part} predominate with respect of R_{ads}, as seen above in Fig. 3.

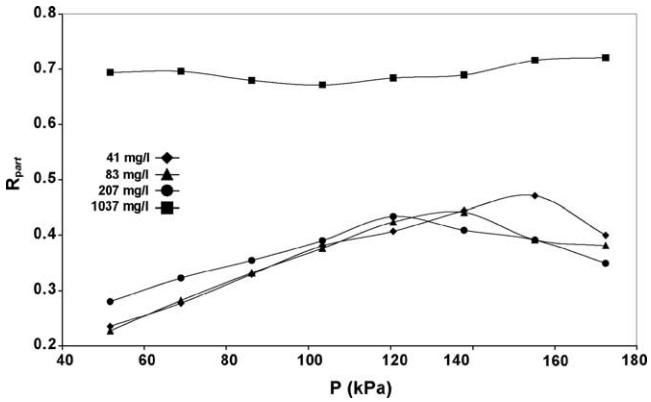

Fig. 5. Values of the ratio between the contribution to the peak area of the partition and the total area, R_{part}, at different concentrations of 1-undecanol *as* a function of the inlet pressure.

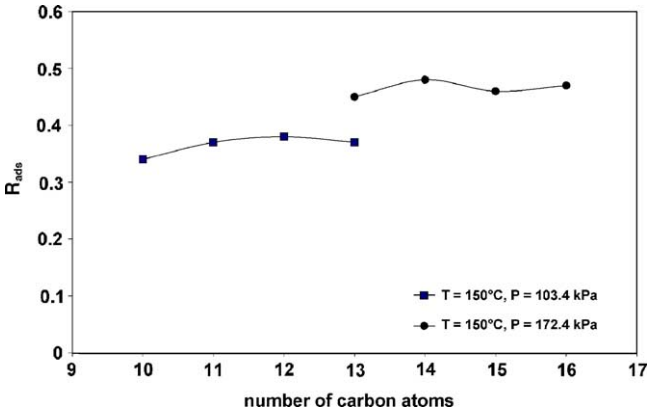

Fig. 6. Values of R_{ads} for 1-alcohols as a function of the number of carbon atoms in the chain. Temperature 150 °C. Inlet pressure 103.4 and 172.4 kPa.

The contribution of the adsorption–desorption phenomena was also investigated as a function of the chain length of the homologous series of 1-alcohols. Fig. 6 shows the values of R_{ads} measured at 103.4 and 172.4 kPa, in order to evaluate a wider range of carbon atoms number. In this instance, the temperature was increased up to 150 °C decreasing to about 20 min the total time of the analysis and obtaining peaks which permit a more accurate determination of their shape. As seen above, the R_{ads} increases with increasing inlet pressure, but is near constant when the length of the chain increases. Therefore, the interaction between the analyte and the active sites due to the hydrogen bonding of the –OH group is much greater than the possible small effect of the increasing length of the hydrocarbon chain. This is confirmed by the fact that no appreciable dependence of the R_{ads} value of the *n*-alkanes on the chain length was observed, because for all the investigated linear alkanes its value was very close to zero.

5. Conclusions

The mathematical model described appears very promising since it gives a fair correspondence between experimental and calculated values of the peak area and of the peak shape, within a wide range of injected sample amount and inlet pressure. The simplified model only takes into account the contribution to the total area of thermodynamic partition and kinetic adsorption–desorption phenomena and does not require complicated convolution integrals. However, it fits very well the peak shape of both non-polar compounds as the hydrocarbons, whose peaks are symmetrical due to the negligible influence of adsorption on the active surface of the column wall, and of polar compounds as the alcohols, which strongly interact with the active silanolic and siloxanic groups of the silica. It is therefore very flexible. The tailing due to the adsorption decreases with increasing the inlet pressure and the carrier gas velocity and shows a minimum value, increasing again at very high inlet pressure. When the injected

amount increases, the adsorption contribution increase linearly up to a concentration of the sample of about 200 mg/l (injected weight about 10 ng); for greater amounts of sample the slope of the adsorption area plot decreases and a plateau is observed, probably due to the saturation of the active centres of the column wall. The shape of the peak due to gas–liquid partition is symmetrical for all of the tested sample concentrations, showing that in the considered range of injected amount (up to about 50 ng) a linear partition isotherm is present. No effect of the chain length was found within the investigated range of carbon atoms number.

References

[1] P. Moretti, S. Vezzani, E. Garrone, G. Castello, J. Chromatogr. A 1038 (2004) 171.
[2] V.B. Di Marco, G.G. Bombi, J. Chromatogr. A 931 (2001) 1.
[3] T.L. Pap, Zs. Papai, J. Chromatogr. A 930 (2001) 53.
[4] Zs. Papai, T.L. Pap, J. Chromatogr. A 953 (2002) 31.
[5] A. Jaulmes, C. Vidal-Madjar, A. Ladurelli, G. Guiochon, J. Phys. Chem. 88 (1984) 5379.
[6] J.C. Giddings, Anal. Chem. 35 (1963) 1999.
[7] A. Villermaux, J. Chromatogr. Sci. 12 (1974) 822.
[8] A. Cavazzini, M. Remelli, F. Dondi, A. Felinger, Anal. Chem. 71 (1999) 3453.
[9] T. Ohkuma, S. Hara, J. Chromatogr. 400 (1987) 47.
[10] F. Dondi, P. Munari, M. Remelli, A. Cavazzini, Anal. Chem. 72 (2000) 4353.
[11] S.C. Pai, J. Chromatogr. A 988 (2003) 233.
[12] S.C. Pai, J. Chromatogr. A 1028 (2004) 89.
[13] O. Kaltenbrunner, A. Jungbauer, S. Yamamoto, J. Chromatogr. A 760 (1997) 41.